Brain Imaging and Behavior
DOI 10.1007/s11682-007-9011-2

Modulation of Resting State Functional Connectivity of the Brain by Naloxone Infusion

Rajan S. Patel · David Borsook · Lino Becerra

Received: 20 July 2007 / Accepted: 26 September 2007

Abstract Recent work regarding the analysis of brain imaging data has focused on examining functional connectivity of the brain. In this paper, we developed and applied a novel framework to examine the modulation of functional connectivity networks during resting state or experimental stimuli. Hierarchical clustering within anatomically parcellated brain regions is used to cluster voxels into anatomically local, functionally homogenous groups. Parcellation allows for the assessment of connectivity at a region of interest level, rather than a voxel-specific level. The framework utilizes a mixed-effects model of the Fisher Z-transformed correlation between pairs of spatially distinct brain regions to assess the modulation of, or differences in, connectivity networks across multiple sessions or between groups of patients. A permutation test was employed to control family-wise type I error. We applied our method to evaluate the effects of a non-selective opioid receptor antagonist, naloxone, on resting state functional connectivity networks with multi-session multi-subject ($n = 10$) functional magnetic resonance imaging data. Naloxone induced a significant reduction in resting state connectivity between the right thalamus and the right parahippocampal gyrus when compared to saline solution.

Keywords fMRI · Functional connectivity · Opioids · Pharmacological · Thalamus · Parahippocampus

R. S. Patel (✉)
Department of Biostatistics, Rollins School of Public Health, Emory University, 1518 Clifton Road, Room 317, Atlanta, GA 30322, USA
e-mail: rajan@alumni.rice.edu

D. Borsook · L. Becerra
Pain Group, McLean Hospital, Harvard University, Cambridge, MA, USA

Introduction

The central nervous system (CNS) consists of billions of interconnected neurons and neuronal ensembles which form the basis of neural processing in the human brain. By studying the interaction of spatially remote interconnected neurons rather than the activation of local neuronal ensembles given particular stimuli, we can more thoroughly understand brain function, as a great deal of neural processing is performed by an integrated network consisting of several regions of the brain.

Functional neuroimaging methods such as functional magnetic resonance imaging (fMRI) allow us to examine relationships between spatially distinct regions of the human brain. One way to assess the relationship between brain regions is by measuring 'functional connectivity'. Friston et al. (1993) define functional connectivity as the 'temporal correlations between spatially remote neurophysiological events'.

Many fMRI studies are often designed to characterize task-induced changes in spatially localized brain activity, however task-free, or resting-state, studies are also conducted to examine a 'default mode' of neural activity (Fox and Raichle 2007). Recent resting-state studies in functional MRI have shown low frequency oscillations (< 0.1 hz) in the temporal signal that are correlated among spatially distributed networks (Cordes et al. 2000). Brain regions involved in these

conscious resting state networks include motor, auditory, visual, and sensorimotor cortices, among others (Peltier et al. 2005). Identifying functional networks in the brain can help to not only examine spatially distinct regions involved in performing various tasks, but also to characterize 'default modes' of the resting state brain. Assessing pharmacological changes in functional connectivity during the resting state can help shed light on the impact of a drug on natural neuronal activity in the brain. For example, Li et al. (2000) examined changes in functional connectivity due to cocaine administration and more recently Anand et al. (2005) assessed changes in connectivity due to antidepressants.

In this paper, we developed and applied a novel framework to examine modulation of or differences in functional connectivity networks during resting state or experimental stimuli. The framework was applied to evaluate the effects of a non-selective opioid receptor antagonist, naloxone, on resting state functional connectivity networks with multi-session fMRI data from healthy volunteers with no history of addiction or opioid exposure. The rationale for using naloxone included the following: (1) it may antagonize basal opioidergic tone in healthy subjects as defined in our paper (for example, post infusion, subjects are more sensitive to mild painful stimuli); (2) it does not have any psychophysical effects that healthy subjects can detect when compared with saline and even at higher doses it has no agonist or intrinsic opioid activity (Aronski et al. 1975).

Naloxone-induced effects on experimental pain have been widely reported but are poorly understood. Some studies report that naloxone increased pain after noxious stimuli (Buchsbaum et al. 1983), whereas others suggest that there is no alteration in pain threshold but an increase in pain-associated anxiety (Grevert and Goldstein 1977, 1978; Stacher et al. 1998). Our group (Borras et al. 2004) previously examined whether naloxone has any effect on normal tonic CNS activity as measured by healthy volunteers with no history of addiction or opioid exposure. We also examined whether prior naloxone administration modulates the effect of mild noxious thermal stimulation on the CNS. We found that naloxone, even in the absence of psychophysical effects, produces activation in several brain regions that are known to have high levels of μ-opioid receptors and may be involved in endogenous analgesia. Understanding naloxone effects on 'default mode' connectivity may help further elucidate its effect on the CNS.

In our previous study, the infusion of naloxone perturbed a 'resting' μ-opioid state with no subjective changes reported by subjects (Borras et al. 2004). The infusion of naloxone produced time courses in the thalamus and parahippocampal/entorrhinal regions that were significantly less correlated than after saline infusion. We interpret these results as a functional interaction between these structures, direct or indirect through inputs from other structures. Although there are now a number of μ-opioid receptor splice variants, it is not known if there is a predominant effect of naloxone on specific regions as a result of receptor density or of μ-opioid specificity. For example, in mice, the μ-opioid receptor gene MOR-1Vi transcript is expressed most highly in the thalamus, hypothalamus and striatum (Doyle et al. 2007).

The connectivity framework described and applied in this paper allows for the examination of changes or differences in connectivity between pairs of spatially localized and functionally homogeneous brain regions. The derivation of the specific measure of connectivity and the parcellation of voxels into spatially localized and functionally homogeneous brain regions is described in detail.

Our approach was as follows: (1) We utilized the anatomical parcellation algorithm devised by Tzourio-Mazoyer et al. (2002) to delineate 98 anatomical parcels from the Montreal Neurological Institute (MNI) template. Each of the 98 parcels was comprised of a group of corresponding voxels from the spatial normalized functional data. (2) Within each of the 98 parcels, we employed average linkage hierarchical clustering (Rencher 2002) of the voxels within each anatomical parcel and the gap statistic stopping rule (Tibshirani et al. 2001) to segregate voxels into functionally homogeneous groups. The resulting clusters yielded volumes of interest (VOI) which served as the units of the examined functional networks. The time series for each VOI is calculated by the mean of the time series of each voxel within the VOI. (3) We constructed a general linear model for each functional scanning session to model effects from external stimuli (when necessary) as well as nuisance effects and extract a residual time series for each VOI. (4) We constructed a mixed effects model of the Fisher Z-transformed correlation between each time series for each pair of VOIs. Doing so allows for the examination of a modulation of connectivity across sessions, groups, or subjects. A permutation test was employed to control family-wise type I error.

Novel contributions of this paper include the development of a framework to examine the modulation of, or difference in, functional connectivity networks of parcellated brain regions that control family-wise type I error and the examination of naloxone induced modulation of resting state functional connectivity of the brain.

Materials and methods

Ten healthy, right-handed, male volunteers (mean age = 31.5 years, standard deviation = 6.6) with no known prior opioid exposure were recruited for this study. Details can be found in Borras et al. (2004).

Subjects participated in two MRI scan sessions one week apart. Naloxone or saline infusions were selected in a randomized, double-blinded, crossover design. Each scan lasted a total of 1,260 s, the first 300 s of which served as a baseline. After 300 s either 4 mg of naloxone or saline solutions were injected over 100 s. The scanning then continued for the remaining 860 s. Only the last 750 s of the post-infusion resting state scans are considered to eliminate any potential acute drug onset effect and such that only steady state pharmacological effects are considered. See Borras et al. (2004) for more information on the experimental paradigm.

A 3 T Siemens scanner with a quadrature headcoil was used to obtain brain images during anatomical and functional scans. Functional scans were acquired continuously in coronal orientation, perpendicular to the AC-PC line and centered around the AC point, with in plane resolution = 3.125 mm, slice thickness = 4 mm, flip angle = 90°, TE = 30 ms and TR = 3.0 s. The field of view covered during functional scans included the entire brain except for the occipital lobe and the posterior cerebellum.

Data pre-processing was carried out using FSL 3.4 software (Center for Functional Magnetic Resonance Imaging of the Brain, University of Oxford, UK; www.fmrib.ox.ac.uk/fsl). Each individual functional scan was registered to its high-resolution anatomical scan and spatially transformed to the MNI 152 template using FLIRT (fMRI linear Image Registration Tool). All volumes were spatially smoothed with a 6mm full width half maximum Gaussian filter. Each volume was anatomically masked with an anatomical template provided by Tzourio-Mazoyer et al. (2002) and proportionally scaled such that the mean of the masked voxels in each volume was 100.

Anatomically local, functional parcellation

We utilized an anatomical parcellation of the MNI template developed by Tzourio-Mazoyer et al. (2002) to group spatially local voxels that correspond to particular brain regions (Fig. 1).

Anatomical parcels ranged in size from 13 voxels to 1,027 voxels. For larger anatomical parcels, it is feasible that there may be functionally heterogeneous clusters of voxels. In 'Determining functional clusters within anatomical parcels', we describe an approach to further divide each anatomical parcel to ensure functional homogeneity within each group of voxels.

Determining functional clusters within anatomical parcels

Previous studies which anatomically parcellate voxels before conducting parcel-wise analyses ignore potential functional heterogeneity of voxels within an anatomical parcel (Salvador et al. 2005). We address this issue by further segregating voxels within anatomical parcels by performing an average linkage agglomerative hierarchical clustering (Rencher 2002) using the gap statistic Tibshirani et al. (2001) to determine the optimal number of clusters.

Average linkage hierarchical clustering

The general objective of functional neuroimaging clustering is to distinguish voxels into k functionally homogeneous clusters that exhibit distinct patterns of measured brain activity. The voxels within individual clusters exhibit similar patterns of neurophysiological response. We describe the functional distance between a pair of voxels, i and j, as the squared Euclidean distance

$$d(i,\, j) = \sum_{p=1}^{P} \sum_{s=1}^{S} \left(\mathbf{Z_{ips}} - \mathbf{Z_{jps}}\right)' \left(\mathbf{Z_{ips}} - \mathbf{Z_{jps}}\right), \tag{1}$$

where Z_{ips} is the temporally de-meaned and variance normalized time series for voxel i during period p for subject s that has dimensionality length T. P is the number of sessions per subject, S is the number of subjects, and T is the number of scans within each session.

The average linkage agglomerative hierarchical clustering algorithm begins with each voxel belonging to its own cluster. Cluster pairs with the smallest distance $d(g, g^*)$ at each iteration are iteratively merged until one cluster remains. $d(g, g^*)$ takes the form

$$\left(N_g^{-1} \times N_{g^*}^{-1}\right) \sum_{i \in \Omega_g} \sum_{j \in \Omega_{g^*}} d(i,\, j), \tag{2}$$

where N_g is the number of voxels in cluster g, and Ω_g is the collection of voxels in cluster g.

The gap statistic

The gap statistic (Tibshirani et al. 2001) is utilized to determine the number of true clusters in the data by comparing the change in within-cluster dispersion with what is expected given a reference null distribution

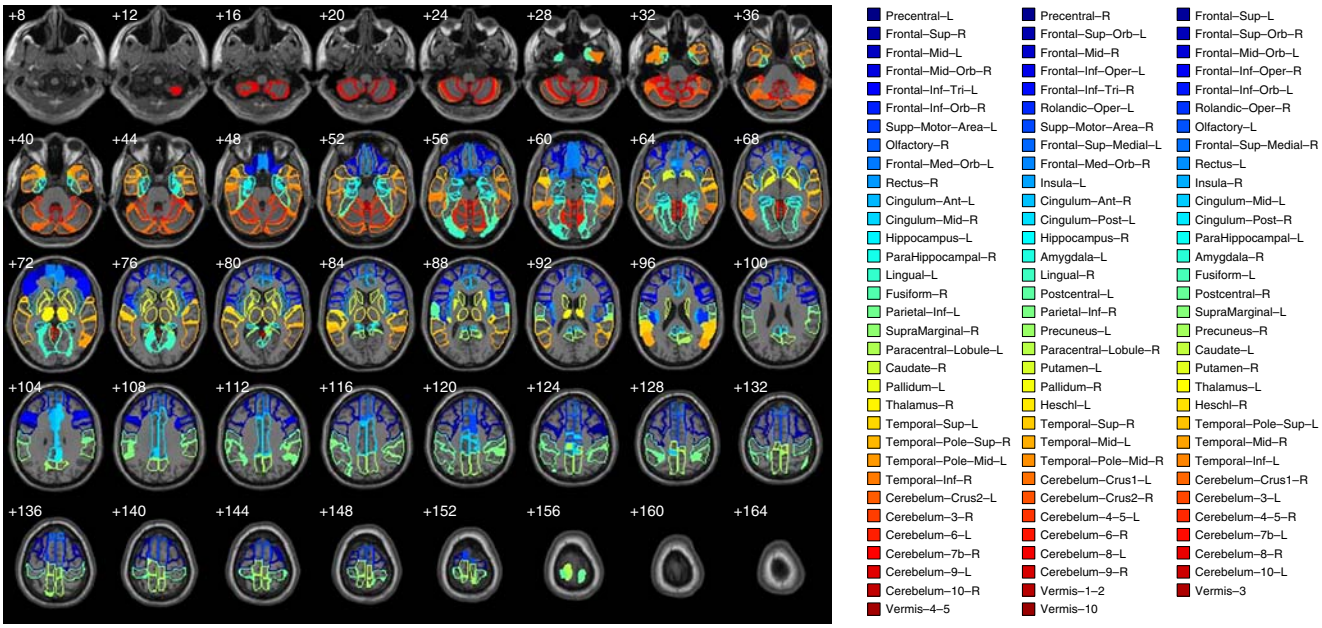

Fig. 1 Regions of interest drawn on axial T1 MNI single-subject slices. Values in upper right corner of each slice represent MNI z coordinate in millimeters

over different numbers of clusters. Since $d(i, j)$ is the squared Euclidean distance between voxels and k is the total number of clusters, then

$$SS_k = \sum_{i=r}^{k} \frac{1}{2N_r} \sum_{i,j \in \Omega_r} d(i, j) \tag{3}$$

is the pooled within-cluster sum of squares around the cluster means. The gap statistic approach standardizes the curves of $\log(SS_k)$ by comparing it with its expectation under the null distribution of the data. The estimate of the optimal number of clusters is the value of k for which $\log(SS_k)$ falls the farthest below the reference curve generated from the null data.

We utilize the principal components based algorithm described by Tibshirani et al. (2001) to generate d reference null data sets and subsequently the expected value of $\log(SS_k)$ under the null, $E_n^*[log(SS_k)]$, where n is the number of observations drawn from the reference distribution. The gap statistic is thus calculated as

$$Gap_n(k) = E_n^* \left[log(SS_k)\right] - log(SS_k). \tag{4}$$

Let $\mathrm{sd}(k)$ be the standard deviation of the d replicates of $\log(SS_k)$. Additionally, to account for the simulation error in $E_n^*[log(SS_k)]$, the standard error of the gap statistic is $s_k = sd(k)\sqrt{1 + 1/d}$. Finally, the optimal number of clusters $\hat{k}$ is the smallest k such that $\mathrm{Gap}(k) \geq \mathrm{Gap}(k+1)$ - s_{k+1}.

Assessing functional connectivity

The specific correlations of interest between two time series from spatially distinct VOIs define the interpretation of functional connectivity for this analysis. We represent each VOI by the average of the time series of the voxels that comprise it. The dimensionality of the data for each session of each subject is $G \times T$ where G is the number of VOIs and T is the number of scans in each session. Our connectivity framework begins with a simple linear model for the time series of each VOI:

$$\mathbf{Y_{sp}(g)} = \mathbf{X_{sp}}\beta_{\mathbf{sp}}(\mathbf{g}) + \mathbf{H_{sp}}\gamma_{\mathbf{sp}}(\mathbf{g}) + \epsilon_{\mathbf{sp}}(\mathbf{g}), \tag{5}$$

where $\mathbf{Y_{sp}(g)}$ is time series of VOI g for subject s and session p, $\mathbf{X_{sp}}$ is the session specific design matrix modeling effects of interest, $\mathbf{H_{sp}}$ is a design matrix modeling nuisance effects (i.e. cardiovascular effects, motion parameters, discrete cosine transforms for removing low frequency drift), and $\epsilon_{\mathbf{sp}}(\mathbf{g})$ is the residual error vector. In this study, effects due to heart rate and respiratory rate were removed during image reconstruction and are thus not included in this model.

For connectivity analyses, the correlation between $\epsilon_{\mathbf{sp}}(\mathbf{g})$ and $\epsilon_{\mathbf{sp}}(\mathbf{g}^*)$ where g and g^* are two spatially distinct VOIs is of interest. The interpretation of $\epsilon_{\mathbf{sp}}(\mathbf{g})$ is determined by the inclusion or exclusion of modeled activations in the $\mathbf{X_{sp}}$ term. Since correlation of the time courses of two active brain regions can be due to a

common input or direct interaction between the two, utilizing the residual time series, i.e. removing modeled activations, or utilizing the detrended time courses provides differing interpretations of the correlation between the time series. Utilizing the residual time series is only appropriate when the modeled activations are equally well captured across the brain and throughout the time series, i.e. no unmodeled attenuation of the BOLD response.

In this study of resting state connectivity, $\mathbf{X_{sp}} = 0$ for all sessions and subjects, and $\mathbf{H_{sp}}$ modeled an intercept and 6 motion parameters, rotation and translation in each of the 3 directions. A least squares estimate of $\gamma_{sp}(g)$ was calculated and thus $\epsilon_{\mathbf{sp}}(\mathbf{g})$ was determined. $\epsilon_{\mathbf{sp}}(\mathbf{g})$ was subsequently low pass filtered for frequencies < 0.1 hz as it was shown by Cordes et al. (2002) that low frequency oscillations in the fMRI time series characterize resting state functional connectivity well.

The Pearson correlation between $\epsilon_{\mathbf{sp}}(\mathbf{g})$ and $\epsilon_{\mathbf{sp}}(\mathbf{g}^*)$, where g and g^* are spatially distinct VOIs is utilized to measure the connectivity between g and g^* for subject s during session p.

Modeling effects on connectivity

Subjects in this study were randomly assigned to receive either naloxone or saline in period 1 and the opposite treatment in period 2. During each period, one post-dose resting state fMRI session was performed. Ten subjects were enrolled in the study, each of whom were examined both under naloxone and saline treatment. The correlation between each pair of VOIs, g and g^*, $\hat{\rho}_{sp}(g, g^*)$, is assessed for each period, p, and subject, s, where $\hat{\rho}_{sp}(g, g^*)$ is the sample Pearson correlation between $\epsilon_{\mathbf{sp}}(\mathbf{g})$ and $\epsilon_{\mathbf{sp}}(\mathbf{g}^*)$.

A naloxone effect on the connectivity between g and g^* is assessed using the following mixed effects model:

$$f(\hat{\rho}_{sp}(g, g^*)) = \mu + \mathrm{per}_p + \mathrm{trt}_t + \mathrm{subj}_s + \nu, \tag{6}$$

where $f(x)$ is the Fisher transformation of x and thus $f(x) = \frac{1}{2}\log\frac{1+x}{1-x}$, per is the fixed period effect, trt is the fixed treatment effect (saline or naloxone), subj is the random subject effect which is distributed as $N(0, D)$, and ν is a residual error term which is distributed as $N(0, \mathbf{V})$. This conditional-independence model is estimated via a restricted maximum likelihood approach where D is a scalar variance parameter and $V = \sigma^2 * \mathbf{I}$. Model estimation was performed using SAS/Proc Mixed software, version 9.1.3 of the SAS System for Windows.

The treatment effect, trt, of naloxone is of interest, thus the t-statistic for the treatment effect is calculated for each pair of VOIs.

A permutation test is used to obtain family-wise type I error corrected p-values for the treatment effect of naloxone. For each of 1000 random permutations of the treatment assignment of each session for each subject, the model in Eq. 6 was fit for each pair of VOIs. For each permutation, we calculated the maximum absolute t-statistic of the treatment effect over each pair of VOIs. By permuting the treatment assignments repeatedly, the null distribution of the maximum t-statistic was obtained. By utilizing the distribution of the maximum absolute t-statistic, we are able to control family-wise Type I error, defined in this case as the probability of rejecting at least one null hypothesis of no treatment effect on connectivity between any pair of VOIs.

For this analysis, we a priori set the probability of Type I error to $\alpha = 0.10$. A treatment effect between any given pair of VOIs is considered statistically significant if the absolute t-statistic of the treatment effect falls above the 90^{th} percentile of the null distribution of the maximum t-statistic.

Simulation to estimate power

We conducted simulated analyses to estimate the power that we have to detect a pair of VOIs with truly modulated connectivity due to treatment. The simulation was performed in the following manner:

- For each of 1,000 iterations, randomly permute the treatment assignment for each session of each subject. Permuting the treatment assignments gives an estimate of the null distribution of the difference in correlations across treatment groups.
- For each iteration, randomly select one pair of VOIs, g and g^*, to have a true difference in correlation. Generate $\epsilon_{\mathbf{sp}}(\mathbf{g})$ and $\epsilon_{\mathbf{sp}}(\mathbf{g}^*)$ for each naloxone session by sampling from a multivariate random normal distribution such that

$$\begin{pmatrix} \epsilon_{\mathbf{sp}}(\mathbf{g}) \\ \epsilon_{\mathbf{sp}}(\mathbf{g}^*) \end{pmatrix} \sim N\left(0, \begin{bmatrix} 1 & \rho \\ \rho & 1 \end{bmatrix}\right). \tag{7}$$

  For each saline session we simulate from independent random normal distributions with unity variance.
- For each iteration, we conduct the permutation test described above and assess whether the connectivity between g and g^* was found to be significantly modulated by naloxone.

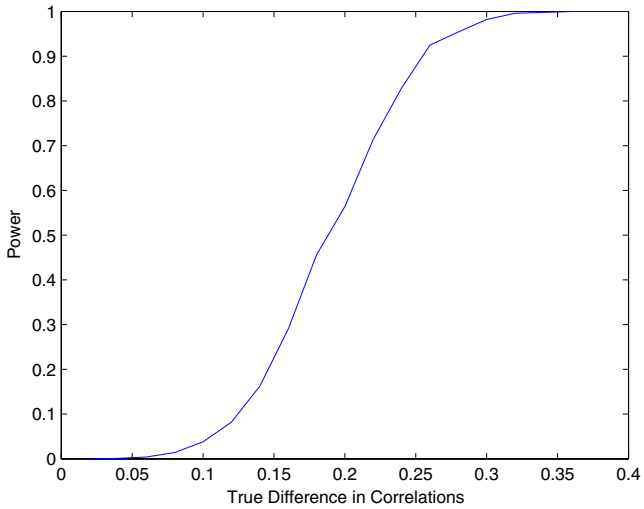

Fig. 2 Power to detect a difference in correlation between treatment groups for a single pair of VOIs at two-sided $\alpha = 0.10$. Results are based on a simulation study assuming that the correlation in the saline group is 0 and the correlation in the naloxone group is ρ

- We repeat the entire procedure for ρ over a range from 0 to 0.4.

We assume for the purpose of this simulation that each subject experiences the same true difference in correlation between pairs of brain regions and that $\epsilon_{\mathbf{sp}}(\mathbf{g})$ is normally distributed. In our simulation, the treatment effect only applies to one randomly select pair of brain regions, the remaining pairs have randomly permuted treatment assignments, and thus no simulated treatment effect. Because we are still conducting hypothesis tests for each pair of brain regions and adjusting for multiple comparisons, power is much lower than it would be if we had restricted ourselves to examining only the selected pair. If we had not conducted multiple tests and controlled for multiple comparisons, the power curve given in Fig. 2 would intersect the y-axis at 0.10, as expected when $\alpha = 0.10$. Our results suggest that we have approximately 83% power to detect a true modulation in correlation of 0.24 at a two-sided Type 1 error level of $\alpha = 0.10$ (Fig. 2).

Results

Hierarchical clustering of anatomical parcels

Hierarchical clustering of the anatomical parcels resulted in 24 of 98 anatomical parcels being further subdivided into 48 functional clusters because of functional heterogeneity, yielding 122 VOIs. The gap statistic suggested that each of the 24 anatomical clusters be subdivided into two subgroups.

Sub-divided anatomical parcels are shown in Fig. 3.

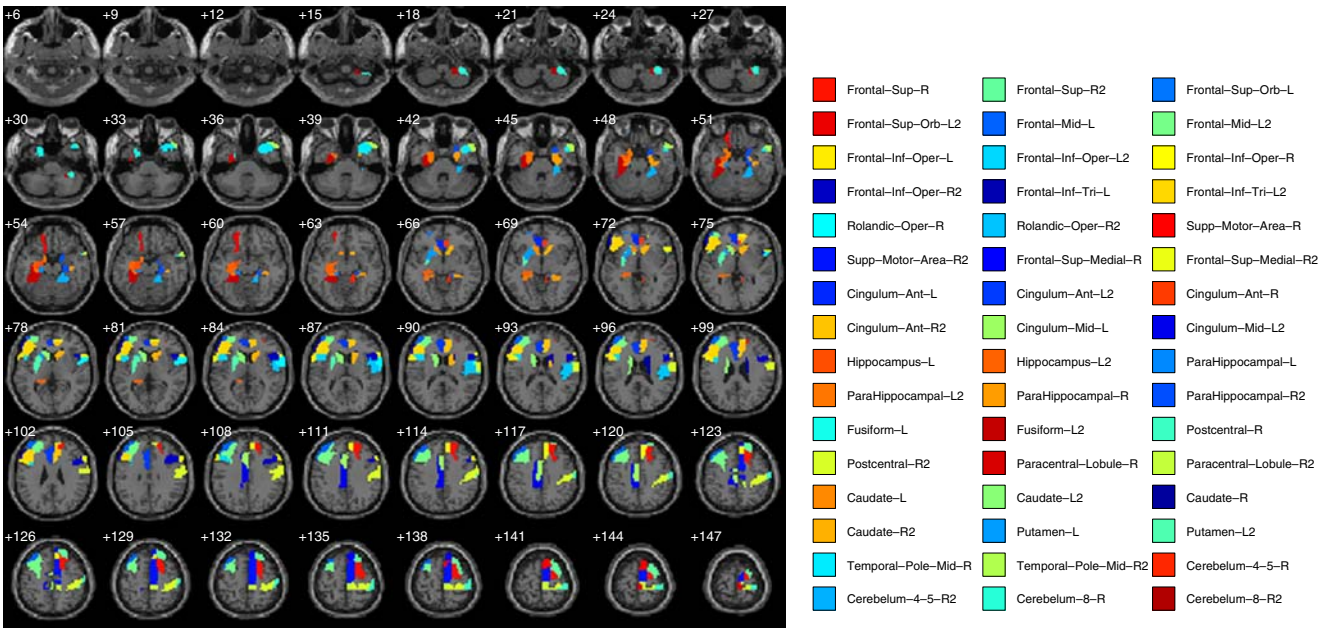

Fig. 3 Anatomical clusters further sub-divided because of more than one functional cluster ($\hat{k} > 1$). A '2' is appended to the name of the second of the two functional subgroups of a particular anatomical cluster

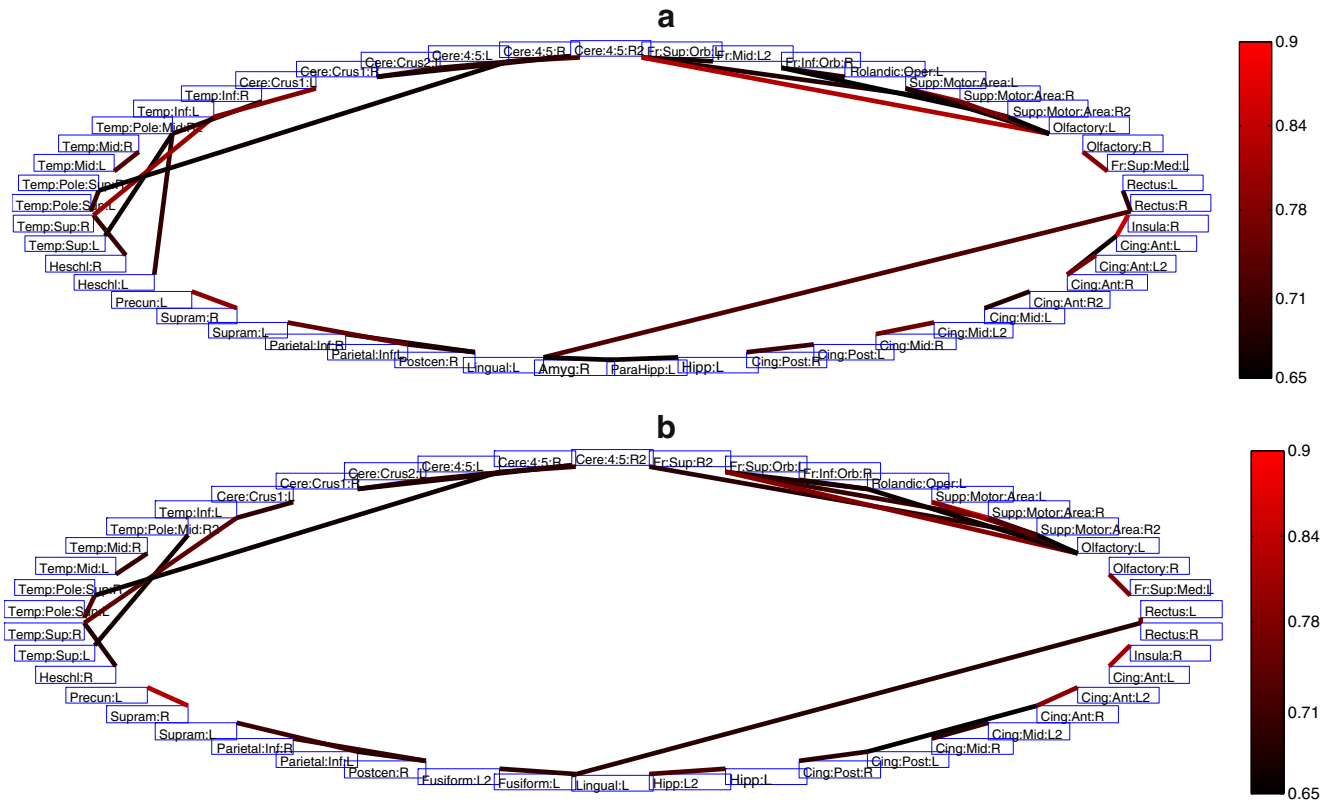

Fig. 4 Strongly correlated pairs of VOIs for saline (**a**) and naloxone (**b**) sessions (threshold correlation > 0.65). The mean correlation for saline (**a**) and naloxone (**b**) sessions over all 10 subjects is shown

Resting state functional networks

Strongly positively correlated pairs of VOIs during resting state for naloxone and saline sessions are shown in Fig. 4. Connections between VOIs are shown if the mean correlation over all 10 subjects was greater than 0.65, which was an arbitrarily chosen cutoff. Networks of positively correlated brain regions are similar for each treatment, with strong bilateral connectivity in the amygdala, lingual gyrus, parahippocampal gyrus, hippocampus, posterior cingulate, insula, gyrus rectus, and thalamus as well as strong intra-regional connectivity in the cerebellum. Additionally strong connectivity between the right posterior cingulate and right precuneus and the putamen and the global pallidus were exhibited under both treatments.

Pairs of VOIs with significant modulation of connectivity by naloxone

The family-wise error ($\alpha = 0.10$) corrected threshold for the t-statistic of the treatment effect of naloxone on connectivity was 6.89. The only pair of brain regions found to have statistically significantly modulated connectivity by naloxone was the right thalamus and the first functional subcluster of the right parahippocampal gyrus (*Parahippocampal-R* in Fig. 3) (t-statistic = −7.41, family-wise corrected p-value = 0.06). Figure 5 visualizes each VOI on a 3D rendering of only the right brain. Absolute correlation between the two regions was significantly decreased when naloxone was administered compared to when saline was administered. A subject by subject plot of the Fisher Z-transformed correlations for naloxone and saline solution scans shows that the correlation between brain regions when naloxone is administered is less than the respective

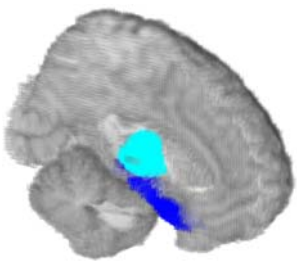

Fig. 5 3D anatomical rendering of the right brain. *Highlighted regions* are the right parahippocampal gyrus (*blue*) and right thalamus (*cyan*)

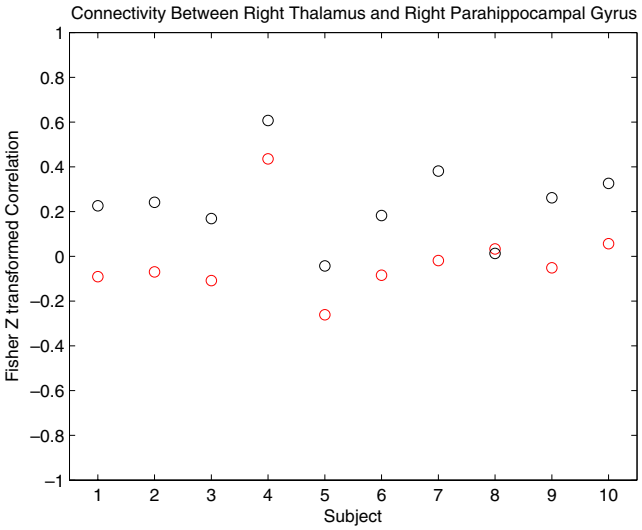

Fig. 6 Subject by subject comparison of connectivity between the right thalamus and the first functional subcluster of the right parahippocampal gyrus for saline (*black*) and naloxone (*red*) sessions

correlation when saline is administered in 9 of 10 subjects (Fig. 6).

Discussion

We observed that naloxone infusion (4 mg) resulted in decreased connectivity strength between the thalamus and in the parahippocampal cortex. No other brain regions were found to have a significant change in correlation. The whole thalamus and the parahippocampal/entorrhinal cortex were included, based on Tzourio-Mazoyer atlas (Tzourio-Mazoyer et al. 2002). Of note, naloxone infusion produced no subjective changes in the subjects compared with the saline infusion (Borras et al. 2004); however, naloxone can alter subjective reports when the system is 'activated', such as pain perception after exercise (Haier et al. 1981). In addition, in our previous naloxone study, the drug also exhibited a subjective and objective (i.e., fMRI) effect in response to heat stimuli (Borras et al. 2004).

Naloxone hydrocholoride ($C_{19}H_{21}NO_4 \cdot HCl$) is a non-selective opioid receptor antagonist, which in fact may have agonist properties for some opioid receptor types. When given intravenously, the onset of action is rapid (within minutes) and the duration of action, while dependent on the dose, and the serum half-life is around 1 h (Berkowitz 1976). The duration of its effects on receptor activity in the human brain is not well defined but in rodents brain levels seem to parallel serum levels (Ngai 1976). Thus, at the time at which the analysis was performed, naloxone had clearly penetrated the brain and bound to opioid receptors.

Opioidergic systems are found throughout the brain and play a significant role in pain and analgesia (Hill 1981), stress response (Drolet et al. 2001), hormonal regulation (Brown et al. 2000), and the placebo response (Benedetti et al. 2005). Our results indicate that naloxone administered in healthy subjects produces a functional decrease in functional connectivity between the thalamus and the hippocampus and parahippocampal cortex. A number of studies have shown opioid binding in the human brain that includes cortical and sub-cortical regions (Baumgartner et al. 2006). Amongst these are the thalamus and hippocampus. It should be noted that Baumgartner et al. (2006) utilized diprenorphine, a non-type selective opioid receptor antagonist, as a radiotracer, labeling all receptor types.

This study did not evaluate connectivity for specific thalamic subnuclei. However, the anterior and mediodorsal thalamic nuclei have connections with the hippocampal regions. A number of studies implicate connectivity between these structures (Aggleton and Pearce 2001). Direct connections between the thalamus and the hippocampus have been described (Linke et al. 2004). Behavioral studies such as lesions of the anterior and mediodorsal thalamic nuclei produce learning impairments in monkeys (Ridley et al. 2002). Such lesions are thought to affect the hippocampal–fornix–thalamic circuit. Positron emission tomography studies using glucose indicate abnormalities in thalamic nuclei in temporal lobe seizure disorders (Juhasz et al. 1999).

Information from unimodal and polymodal association cortices enters the MTL through the perirhinal and parahippocampal cortices, which project to the entorhinal cortex, which in turn provides the major input to the hippocampal formation. Thus, the regions are associated with incoming sensory information. The hippocampal formation is not only important in transfer of information between sensory and motor association areas, but is also involved in connections implicated in endocrine and autonomic functions (Braak et al. 1998). Thus, it plays a role in integrating both exteroceptive sensory- and interoceptive autonomic-information. The implication of the naloxone-induced reduction in connectivity between the thalamus and hippocampus is not fully understood, however our hypothesis is that this reduction in connectivity would result in a reduced flow of sensory and motor information as both regions play a role in the relay of information selectively to various parts of the cortex.

Caveats

Given that endogenous opioid systems are so diverse and found throughout the CNS, it is perhaps surprising that no other changes in connectivity were observed. This may be for a number of reasons including: (1) They do not exist, which seems unlikely given the known connectivity with regions such as prefrontal regions and the amygdala (Roberts et al. 2007) or hypothalamus (Floyd et al. 2001), areas that also have high levels of μ-opioid receptors. (2) The duration of the infusion used for the analysis was only 8 min and perhaps there is a delayed effect, which was not evaluated. (3) We did not assess a dose dependent response that may increase power to define other regions that show significant changes in connectivity.

Conclusion

We developed and applied a novel framework for examining changes due to some intervention or differences between groups of subjects in functional connectivity between pairs of functionally homogeneous and spatially local brain regions. The framework provides a method to parcellate voxels into spatially local and functionally homogeneous brain regions, a model for how connectivity can be defined, and a method to properly adjust for multiple comparisons.

The association of the thalamic region with the parahippocampal/entorrhinal region may have implications in the clinical condition. For example, in chronic neuropathic pain there is a decrease in opioid receptor binding a number of regions including the thalamus (Jones et al. 2004). Such connectivity studies may provide useful insights into neural systems processing in health and disease.

References

Aggleton, J., & Pearce, J. (2001). Neural systems underlying episodic memory: insights from animal research. *Philosophical Transactions of the Royal Society of London. Series B, Biological Sciences, 356*, 1467–1482.

Anand, A., Li, Y., Wang, Y., Wu, J., Gao, S., Bukhari, L., et al. (2005). Antidepressant effect on connectivity of the mood-regulating circuit: An fmri study. *Neuropsychopharmacology, 30*, 1334–1344.

Aronski, A., Kubler, A., Majda, A., & Jakubaszko, J. (1975). Comparative study of the action of naloxone (narcan) and nalorphine in man. *Anaesthesia, Resuscitation and Intensive Therapy, 3*, 221–230.

Baumgartner, U., Buchholz, H., Bellosovich, A., Margerl, W., Siessmeier, T., Rolke, R., et al. (2006). High opiate receptor binding potential in the human lateral pain system. *NeuroImage, 30*, 692–699.

Benedetti, F., Mayberg, H., Wager, T., Stohler, C., & Zubieta, J. K. (2005). Neurobiological mechanisms of the placebo effect. *Journal of Neuroscience, 45*, 10390–10402.

Berkowitz, B. (1976). The relationship of pharmacokinetics to pharmacological activity: Morphine, methadone and naloxone. *Clinical Pharmacokinetics, 1*, 219–230.

Borras, M., Becerra, L., Ploghaus, A., Gostic, J., DaSilva, A., Gonzalez, R., et al. (2004). Fmri measurement of cns responses to naloxone infusion and subsequent mild noxious thermal stimuli in healthy volunteers. *Journal of Neurophysiology, 91*, 2723–2733.

Braak, H., Braak, E., Yilmazer, D., & Bohl, J. (1998). Functional anatomy of human hippocampal formation and related structures. *Journal of Child Neurology, 13*, 146–147.

Brown, C., Russell, J., & Leng, G. (2000). Opioid modulation of magnocellular neurosecretory cell activity. *Neuroscience Research, 36*, 97–120.

Buchsbaum, M., Davis, G., Naber, D., & Pickar, D. (1983). Pain enhances naloxone-induced hyperalgesia in humans as assessed by somatosensory evoked potentials. *Psychopharmacology, 79*, 99–103.

Cordes, D., Haughton, V., Arkanakis, K., Wendt, G., & Turski, P. (2000). Mapping functionally related regions of brain with functional connectivity mri (fcmri). *American Journal of Neuroradiology, 21*, 1636–1644.

Cordes, D., Haughton, V., Carew, J., Arfanakis, K., & Maravilla, K. (2002). Hierarchical clustering to measure connectivity in fMRI resting-state data. *Magnetic Resonance Imaging, 20*, 305–317.

Doyle, G., Sheng, R., Lin, S., Press, D., Grice, D., Buono, R., et al. (2007). Identification of three mouse mu-opioid receptor (mor) gene (oprm1) splice variants containing a newly identified alternatively spliced exon. *Gene, 388*, 135–147.

Drolet, G., Dumont, E., Gosselin, I., Kinkead, R., Laforest, S., & Trottier, J. (2001). Role of endogenous opioid system in the regulation of the stress response. *Progress in Neuropsychopharmacol Biological Psychiatry, 25*, 729–741.

Floyd, N., Price, J., Ferry, A., Keay, K., & Bandler, R. (2001). Orbitomedial prefrontal cortical projections to hypothalamus in the rat. *Journal of Comparative Neurology, 432*, 307–328.

Fox, M., & Raichle, M. (2007). Spontaneous fluctuations in brain activity observed with functional magnetic resonance imaging. *Nature Reviews Neuroscience, 8*, 700–711.

Friston, K., Frith, C., Liddle, P., & Frackowiak, R. (1993). Functional connectivity: the principal component analysis of large (PET) data sets. *Journal of Cerebral Blood Flow and Metabolism, 13*, 5–14.

Grevert, P., & Goldstein, A. (1977). Effects of naloxone on experimentally induced ischemic pain and on mood in human subjects. *Proceedings of the National Academy of Sciences of the United States of America, 74*, 1291–1294.

Grevert, P., & Goldstein, A. (1978). Endorphins: naloxone fails to alter experimental pain or mood in humans. *Science, 199*, 1093–1095.

Haier, R., Quaid, K., & Mills, J. (1981). Naloxone alters pain perception after jogging. *Psychiatry Research, 5*, 231–232.

Hill, R. (1981). Endogenous opioids and pain: A review. *Journal of the Royal Society of Medicine, 74*, 448–450.

Jones, A., Watabe, H., Cunningham, V., & Jones, T. (2004). Cerebral decreases in opioid receptor binding in patients with central neuropathic pain measured by [11C]diprenorphine binding and pet. *European Journal of Pain, 8*, 479–485.

Juhasz, C., Nagy, F., Watson, C., da Silva, E., Muzik, O., Chugani, D., et al. (1999). Glucose and [11C]flumazenil positron emission tomography abnormalities of thalamic nuclei in temporal lobe epilepsy. *Neurology, 53*, 2037–2045.

Li, S., Biswal, B., Li, Z., Risinger, R., Rainey, C., Cho, J., et al. (2000). Cocaine administration decreases functional connectivity in human primary visual and motor cortex as detected by functional mri. *Magnetic Resonance in Medicine, 43*, 45–51.

Linke, R., Faber-Zuschratter, H., Seidenbecher, T., & Pape, H. (2004). Axonal connections from posterior paralaminar thalamic neurons to basomedial amygdaloid projection neurons to the lateral entorhinal cortex in rats. *Brain Research Bulletin, 63*, 461–469.

Ngai, S. (1976). Pharmacokinetics of naloxone in rats and in man: Basis for its potency and short duration of action. *Anesthesiology, 44*, 398–401.

Peltier, S., Kerssens, C., Hamann, S., Sebel, P., Byas-Smith, M., & Hu, X. (2005). Functional connectivity changes with concentration of sevoflurane anesthesia. *Neuroreport, 16*, 285–288.

Rencher, A. (2002). Methods of multivariate analysis (2nd ed.). New York: Wiley.

Ridley, R., Maclean, C., Young, F., & Baker, H. (2002). Learning impairments in monkeys with combined but not separate excitotoxic lesions of the anterior and mediodorsal thalamic nuclei. *Brain Research, 950*, 39–51.

Roberts, A., Tomic, D., Parkinson, C., Roeling, T., Cutter, D., Robbins, T., et al. (2007). Forebrain connectivity of the prefrontal cortex in the marmoset monkey (callithrix jacchus): an anterograde and retrograde tract-tracing study. *Journal of Comparative Neurology, 502*, 86–112.

Salvador, R., Suckling, J., Coleman, M., Pickard, J., Menon, D., & Bullmore, E. (2005). Neurophysiological architecture of functional magnetic resonance images of human brain. *Cerebral Cortex, 15*, 1332–1342.

Stacher, G., Abatzi, T., Schulte, F., Schneider, C., Stacher-Janotta, G., Gaupmann, G., et al. (1998). Naloxone does not alter the perception of pain induced by electrical and thermal stimulation of the skin in healthy humans. *Pain, 34*, 271–276.

Tibshirani, R., Walther, G., & Hastie, T. (2001). Estimating the number of clusters in a data set via the gap statistic. *Journal of the Royal Statistical Society. Series B. Methodological, 63*, 411–423.

Tzourio-Mazoyer, N., Landeau, B., Papathanassiou, D., Crivello, F., Etard, O., Delcroix, N., et al. (2002). Automated anatomical labeling of activations in SPM using a macroscopic anatomical parcellation of the mni mri single-subject brain. *NeuroImage, 15*, 273–289.